Fredrik Gustafsson and Fredrik Gunnarsson

© DIGITALVISION

Mobile Positioning Using Wireless Networks

Possibilities and fundamental limitations based on available wireless network measurements

Positioning in wireless networks is today mainly used for yellow page services. Yet, its importance will grow when emergency call services become mandatory as well as with the advent of more advanced location-based services and mobile gaming. It is also plausible that future resource management algorithms may rely on position estimation and prediction. In this article, we discuss and illustrate possibilities and fundamental limitations associated with mobile positioning based on available wireless network measurements. The possibilities include a sensor fusion approach and model-based filtering, while the fundamental limitations provide hard bounds on the accuracy of position estimates, given the information in the measurements in the most favorable situation. The focus is on illustrating the relation between performance requirements, such as those stated by the Federal Communications Commission (FCC), and the available measurements. Specific issues on accuracy limitation in each measurement, such as synchronization and multipath problems, are only briefly commented upon. A geometrical example, as well as a realistic example adopted from a cell planning tool, are used for illustration.

MOBILE POSITIONING
Various location-based services in wireless communication networks depend on mobile positioning. Commercial examples range from low-accuracy methods based on cell identification

[TABLE 1] FCC REQUIREMENTS FOR MOBILE AND NETWORK-CENTRIC POSITIONING, RESPECTIVELY, EXPRESSED IN CIRCULAR ERROR PROBABILITY (CEP). [FOR INSTANCE CEP67=100 M MEANS THAT AT LEAST 67% OF THE RADIAL POSITIONING ERRORS ARE SMALLER THAN 100 M.]		
SPECIFICATION	NETWORK-CENTRIC	MOBILE-CENTRIC
CEP67	FCC-N 1: 100 M	FCC-M 1: 50 M
CEP95	FCC-N 2: 300 M	FCC-M 2: 150 M

to high-accuracy methods combining wireless network information and satellite positioning. These methods are typically *network centric*, where the position is determined in the network and presented to the user via a specific service. Due to logistical reasons, the position is estimated from static snapshot measurements, possibly provided by the mobile station (MS). *Mobile-centric* solutions enable the use of sampled temporal measurements and motion models to enhance estimation accuracy and integrity. Measurements either explicitly or implicitly relate the MS position to the position of reference points (RP) (e.g., positions of radio base stations or satellites) or to the specific behavior of the MS and its surrounding environment. Measurements are typically directional, such as the angle of arrival (AOA) between MS and RP, or related to relative distances, such as the time of arrival (TOA), time difference of arrival (TDOA), and received signal strength (RSS). The survey articles [1]–[5] provide further information about positioning in wireless networks and associated standardization. Indoor positioning includes its own specific challenges and is discussed in [6]. Localization based on ultra-wideband (UWB) radios is particularly suitable for limited range positioning, and is discussed in [7]. Another related area is sensor cooperative localization [8], which is integral to sensor networks positioning.

While yellow page services require only crude position estimates (such as cell identity), more advanced services like mobile gaming could benefit from accurate and timely position estimates. Furthermore, the emergency call accuracy requirements by the FCC have been tightened recently [9], as summarized in Table 1 [2].

Therefore, it is of interest to discuss the achievable accuracies of the different methods. With the introduction of MS with built-in global positioning system (GPS) receivers, the required accuracy is achieved with margin for these applications in outdoor situations. However, GPS still needs support in urban and indoor situations. Furthermore, it will take a long time for full market penetration of MS with GPS, so network-centric solutions cannot rely on GPS for quite a while.

This tutorial-oriented article focuses on positioning based on uncertain measurements. In essence, position estimation is interpreted as a problem of solving systems of nonlinear equations. The accuracy of the solution is related to the information in the measurements through the Fisher information matrix (FIM). This provides a general basis for analyzing sensor configuration and sufficiency of information for specific accuracy requirements. The static case can be approached by either applying a stochastic gradient algorithm or by numerically approximating the nonlinear least-squares problem using Monte Carlo-based techniques. The latter method can also be applied to the dynamic case with a motion model of the mobile. This method is more generally applicable to such information as digital map information. The described methods apply to general wireless network measurements, but specific applications will be exemplified.

This article does not cover low-layer issues related to the actual implementation of the wireless communication network, which usually are limited by the corresponding standard. Of course, many important limitations on positioning can be found here. For instance, the resolution in AOA depends on antenna configuration. Timing measurements such as TOA and TDOA rely on synchronization and correlation techniques applied to known training sequences or pilot symbols. During line-of-sight (LOS), a rule of thumb is that timing can be achieved down to a fraction of the chip duration. Furthermore, non-line-of-sight (NLOS) causes information loss in all these measurements. These issues imply fundamental accuracy limitations that, to a large extent, depend on the system specification; to explain all this in detail is outside the scope of this article. An extensive overview can be found in [10] and the references therein. However, some related survey papers are quoted to give a rough idea of what the accuracy is in practice, and we briefly comment on how NLOS and synchronization influence achievable position accuracy.

MEASUREMENTS

This section provides an overview of different categories of measurements that can be found in most wireless communication systems. System-specific, low-layer techniques for how these are computed are not explained, and more details on this can be found in [3] and [11] for second-generation (2G) and [2] and [10] for third-generation (3G), respectively. Also, [12] provides an overview of error sources in general systems.

Denote the two-dimensional (2-D) mobile position at time t by $p_t = (X_t, Y_t)^T$, and the known base station (BS) positions by $p_t^i = (X_t^i, Y_t^i)^T$. The base stations can, in general, move in time, as is the case in some ad-hoc networks and sensor networks problems. A generic measurement y_t^i relative to reference point i is a function $h_{\text{type}}(p_t, p_t^i)$ of both mobile position and BS position, and it is subject to an uncertainty e_t^i.

MEASUREMENT CATEGORIES
Typical measurements are summarized below. All measured times are in the sequel multiplied by the speed of light to get a measure in meters rather than in nanoseconds.

■ *RSS:* $y_t^i = h_{\text{RSS}}(|p_t - p^i|) + e_t^i$. The transmitter and received power are known to the system, so the channel attenuation (which increases with distance) can be computed. The attenuation is averaged over fast fading and depends on distance and slow fading. A model that solely depends on the relative distance is the so-called Okumura-Hata model [13]–[14] $y_t^i = K - 10\alpha \log_{10} \ (|p_t - p^i|) + e_t^i$,

where $\text{std}(e_t^i) \approx 4 - 12$ dB depending on the environment (desert to dense urban). It is also possible to utilize a predicted or measured spatial digital map with RSS values, as shown in the power map illustrated in Figure 1.

■ *TOA:* $y_t^i = |p_t - p^i| + e_t^i = h_{\text{TOA}}(p_t, p^i) + e_t^i$. The signal's travel time can be computed in a completely synchronized network. Usually, the MS clock is not synchronized, so its clock bias must be treated as a nuisance parameter. This is the case in the GPS where only the satellites are synchronized. Travel time can be measured in many different ways. For example, it is estimated in the uplink to GSM at multiple BSs upon the request of the network. The performance depends mainly on the synchronization accuracy, which in turn is limited by the chip rate. GPS typically features an accuracy of about 10 m in unobstructed environments, while 2G and 3G systems have an achievable accuracy in the neighborhood of 100 m.

The 3G systems will feature assisted GPS, where required information for measurement setup and positioning calculations are broadcast in each cell by the BSs in the cellular network. This approach improves reliability and reduces time to position fix.

■ *TDOA:* $y_t^{i,j} = |p_t - p^i| - |p_t - p^j| + e_t^i - e_t^i = h_{\text{TDOA}}(p_t, p^i, p^j) + e_t^i - e_t^i$. Taking time differences of TOA measurements eliminates the clock bias nuisance parameter. It is a practical mobile measurement related to relative distance. The measurements are reported to the network, which performs necessary computations. With this approach, it is not necessary to communicate the network synchronization nor the reference point locations to the mobile. As for TOA, the synchronization accuracy determines the performance but also the BS locations. The observed TDOA accuracy requirement for location purposes in WCDMA is 0.5 chip [2] which translates to an error of about 40 m ($\sigma_e \approx 20$ m). Similarly, a TDOA accuracy requirement of 0.5 chip in cdma2000 [advanced forward link trilateration (A-FLT)] means 120 m ($\sigma_e \approx 60$ m) due to the lower chip rate. On the other hand, satellite navigation systems have a much higher chip rate, such that assisted GPS can provide TDOA measurements with $\sigma_e \approx 1$ m.

■ *AOA:* $y_t^i = h_{\text{AOA}}(p_t, p^i) + e_t^i$. The use of directionally sensitive antennas provides AOA information. Today, it is mainly available as very crude sector information (e.g., 120° for a three-sector antenna as illustrated in Figure 1). With the use of group antennas, this will be improved to about 30° beam width ($\sigma_e \approx 8°$) and perhaps even better. Geometrically, the spatial resolution of the intersection of two perfectly complementing AOA measurements is limited to $2D\sin(\alpha/2)$, where α is the angular resolution and D is the

distance between the antennas. For $\alpha = 30°$, this means 36% of D.

■ *Digital map information:* $y_t = h_{\text{MAP}}(p_t, p^i) + e_t$. A digital map contains, for instance, RSS measurements relative the reference points either predicted or provided via dedicated measurement scans in the service area. The former is conducted in the network deployment phase using graphical information systems dedicated to network planning, like the TEMS CellPlanner Universa (http://www.ericsson.com/tems/) by Ericsson. The size of the prediction grid is usually from 100 m down to a few meters when considering building data. Figure 1 illustrates such digital prediction maps. Performing actual measurements is only plausible in very limited service areas, like in indoor environments. Most of the shadowing is included in the maps, and the remaining shadow fading component has typically $\text{std}(e_t^i) \approx 3$ dB depending on the environment and spatial map resolution. The map can also be a commercial street map for automotive terminals [15], as examplified in Figure 1. GPS support for sea navigation was proposed in [16] using sonar depth measurements and a depth map.

■ *Position estimates:* $y_t = p_t + e_t$. A direct position estimate may be available, for instance from GPS. Typical accuracy without differential support is on the order of 5–10 m.

Note that GPS positioning can be incorporated either as a position estimate with estimated error statistics or as the actual TOA measurements fused together with other measurements. Table 2 summarizes the discussed measurement categories. It is possible to derive Cramér-Rao bounds (CRBs)
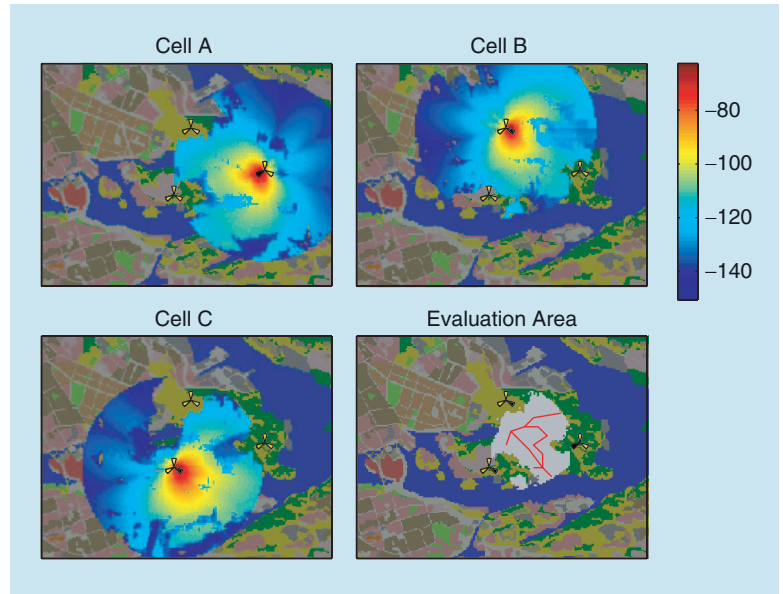
[FIG1] An example of RSS predictions with the spatial resolution 40 m using TEMS CellPlanner Universal. The artificial network is deployed at Djurgården, Stockholm, Sweden (true terrain data, and fictitious but realistic base station locations). Three base stations are indicated with propeller-like symbols in the figures, where each one contains a three-sector antenna. The power gain map from one sector in one base station is illustrated. The evaluation area used in examples is the shaded area in the last plot, where all three BS can be detected. A simple and artificial road map is also depicted.

for the accuracy in each category as a function of system and environment parameters (see [7] for some examples). However, our starting point is to use available information in a network and determine the accuracy of positioning based on this information. That is, the noise standard deviation values in parantheses indicate values used in numerical evaluations and represent favorable situations with essentially LOS measurements. For more detailed discussions regarding measurement accuracies for TOA/TDOA, see [17]–[20]; for AOA, see [21]; and for RSS, see [22] and [23]. Note that the quality of the sensor information depends not only on the noise variance but also on the size and variation in $h(p)$. This is discussed in a later section on performance bounds.

ERROR MODELS

The accuracy levels indicated in Table 2 are based on several assumptions. First, the timing measurements are based on synchronization techniques. In GSM for instance, a 26-b known training sequence in each burst is found by correlation. The bit duration is about 554 m, but using continuous time techniques, time synchronization down to a fraction (say 100 m) is possible. Similar figures hold for the 3G standard universal mobile telecommunications system (UMTS), where the travel time is estimated using the first detected ray in the RAKE algorithm from the known pilot symbols. The computed time estimates are assumed to be unbiased, with a standard deviation σ. In many cases, a Gaussian distribution can be motivated by asymptotic arguments or the central limit theorem, so we can assume

$$p_E(e_t) = \mathrm{N}(0, \sigma^2), \tag{1a}$$

where $\mathrm{N}(0, \sigma^2)$ is short-hand notation for the Gaussian probability density function (pdf) $p_E(e_t) = (2\pi\sigma^2)^{-1/2}e^{-(e_t^2/2\sigma^2)}$. If this is not the case, the Gaussian distribution is the least informative distribution for a given variance [24], so the lower bounds to be computed still hold for estimation and filtering algorithms based on the Gaussian assumption. However, some of the algorithms in the following sections can make use of any pdf for e_t, thus reducing the attainable lower bounds.

An important assumption for all time measurements is LOS. In an NLOS situation, the time estimate will get a positive bias μ and probably another (larger) variance

$$p_E(e_t) = \mathrm{N}(\mu, \sigma_{\mathrm{NLOS}}^2). \tag{1b}$$

The problem here is that we cannot easily detect NLOS. One solution is to use robust algorithms. Another approach is to model the error distribution with a mixture, for instance the two-mode Gaussian mixture

$$p_E(e_t) = \alpha\mathrm{N}(0, \sigma_{\mathrm{LOS}}^2) + (1 - \alpha)\mathrm{N}(\mu, \sigma_{\mathrm{NLOS}}^2), \tag{1c}$$

where $(\alpha, \mu, \sigma_{\mathrm{LOS}}, \sigma_{\mathrm{NLOS}})$ are free parameters in the distribution. Here, e_t falls in the LOS distribution with probability α and the NLOS distribution with probability $1 - \alpha$. Algorithms based on this distribution will automatically be more robust than algorithms that do not model NLOS.

Only TOA and TDOA are discussed above, but similar mixtures are suitable to use also for AOA, where NLOS again increases variance.

Another important aspect of the dynamic case with temporal measurements is that TOA, TDOA, and AOA measurements are highly correlated in time. To use these measurements in a filter, the filter update rate should be matched to their coherence time.

STATIC CASE

In the sequel, all available measurements at time t are collected in the vector y_t, which is related to the mobile position p_t by $y_t = h(p_t) + e_t$. The BS position is from now on implicit in $h(p_t)$. That is, the vector y_t can consist of any combination of information in Table 2, and its size can change over time.

In the static case, there is no assumption of temporal correlation of the position, so the position vector is a sequence of uncorrelated parameters estimated in a snap-shot manner. Knowledge of measurement error distributions can improve the performance, and Cramér-Rao lower bounds (CRLBs) serve as fundamental performance limits.

ESTIMATION CRITERIA

The general positioning challenge is to find the position that minimizes a given norm of the difference of actual measurements and the measurement model. Using the minimizing argument notation for a general loss function $V(p)$, we have

$$\hat{p} = \arg\min_p V(p) = \arg\min_p \|y_t - h(p)\|. \tag{2}$$

The most common choices of norms are discussed below and summarized in Table 3.

[TABLE 2] MATHEMATICAL NOTATION OF AVAILABLE MEASUREMENTS IN WIRELESS COMMUNICATION SYSTEMS TOGETHER WITH APPROXIMATIVE NOISE STANDARD DEVIATIONS σ_e. [HERE y IS THE ACTUAL NUMERICAL VALUE, h DENOTES A GENERAL NONLINEAR MODEL, p_t IS THE SOUGHT POSITION, p^i DENOTES THE POSITION OF BASE STATION/ANTENNA NUMBER i AND e DENOTES MEASUREMENT NOISE WITH A PROBABILITY DENSITY FUNCTION $p_E(\cdot)$.]

TYPE OF MEASUREMENT	NOTATION	ACCURACY
RECEIVED SIGNAL STRENGTH	$y_t^i = h_{\mathrm{RSS}}(\|p_t - p^i\|) + e_t^i$	4–12 dB (10 dB)
TIME OF ARRIVAL	$y_t^i = \|p_t - p^i\| + e_t^i = h_{\mathrm{TOA}}(p_t, p^i) + e_t^i$	5–100 M (14 M)
TIME DIFFERENCE OF ARRIVAL	$y_t^{i,j} = \|p_t - p^i\| - \|p_t - p^j\| + e_t^{ij} = h_{\mathrm{TDOA}}(p_t, p^i, p^j) + e_t^{ij}$	10–60 M (20 M)
ANGLE OF ARRIVAL	$y_t^i = h_{\mathrm{AOA}}(p_t, p^i) + e_t^i$	$5^o - 10^o$ (6°)
DIGITAL MAP INFORMATION	$y_t = h_{\mathrm{MAP}}(p_t) + e_t$	(RSS MAP, 3 dB)
POSITION ESTIMATES (E.G., GPS)	$y_t = p_t + e_t$	5–20 M

Table 3 starts with the nonlinear least-squares criterion. In a stochastic setting where the measurements are subject to a stochastic unknown error e_t, optimizing the 2-norm is the best approach if the errors are independent, identically distributed Gaussian variables; that is, $p_E(e_t) = \mathrm{N}(0, \sigma_e^2 I)$. If there is a spatial correlation, or if the measurements are of different quality over time or for different sensors, improvements are possible. In these cases where $\mathrm{Cov}(e_t) = R_t$, the weighted NLS is preferred. Further, with a given error probability distribution $p_E(e)$, the maximum likelihood (ML) approach provides an efficient estimator. In the special case of a Gaussian error distribution with position-dependent covariance $p_E(e_t) = \mathrm{N}(0, \mathrm{R}(p_t))$, the ML criterion is similar to the WNLS criterion, but with the term $\ln \det R_t(p)$. This term prevents the selection of positions with large uncertainty (large $\mathrm{R}(p_t)$), which could be the case with WNLS.

POSITION ESTIMATION

In the general case, there is no closed-form solution to (2). One exception is an interesting reformulation of the nonlinear least-squares problem. It is demonstrated in [25] that by including an auxiliary parameter for the absolute distance from the MS to an arbitrary reference BS, the NLS problem can be rewritten as a linear least-squares problem where there is an additional constraint on the position and the auxiliary parameter. In this manner, there are no local minima in the loss function. See [5] for a nice summary of explicit least-squares formulations.

In the general case, however, a numerical search method is needed. As in any estimation algorithm, the classical choice is between a gradient and Gauss-Newton algorithm [26]. The basic forms are given in Table 4. These local search algorithms generally require good initialization; otherwise, the risk is to reach a local minimum in the loss function $V(p)$. The least-squares formulation above may provide an adequate initialization. Today, simulation-based optimization techniques may provide an alternative. For further illustrations on computing the ML estimate for TDOA measurements, see [27] and [28].

FUNDAMENTAL PERFORMANCE BOUNDS

The FIM provides a fundamental estimation limit for unbiased estimators referred to as the CRLB [29]. This bound has been analyzed thoroughly in the literature, primarily for AOA, TOA, and TDOA [18], [30]–[34], but also for RSS [23], [35] and with specific attention to the impact from NLOS [36], [37].

[TABLE 3] OPTIMIZATION CRITERIA $V(p)$ FOR ESTIMATING POSITION p FROM UNCERTAIN MEASUREMENTS $y = h(p) + e$ USING (2). [THE VECTOR ELEMENTS IN y AND $h(p)$ COME FROM TABLE 2.]

NONLINEAR LEAST SQUARES	NLS	$V^{\mathrm{NLS}}(p) = \|y_t - h(p)\|^2 = (y_t - h(p))^T(y_t - h(p))$
WEIGHTED NONLINEAR LEAST SQUARES	WNLS	$V^{\mathrm{WNLS}}(p) = (y_t - h(p))^T R_t^{-1}(p)(y_t - h(p))$
MAXIMUM LIKELIHOOD	ML	$V^{\mathrm{ML}}(p) = \log p_E(y_t - h(p))$
GAUSSIAN ML	GML	$V^{\mathrm{GML}}(p) = (y_t - h(p))^T R_t^{-1}(p)(y_t - h(p)) + \log \det R_t(p)$

[TABLE 4] ESTIMATION ALGORITHMS APPLICABLE TO OPTIMIZATION CRITERIA IN TABLE 3. [HERE, $R = I$ FOR NLS AND ML, $H(p) = \nabla_p h(p)$ FOR NLS AND WNLS AND $H(p) = \nabla_p \ln p_E(y - h(p))$ FOR ML.]

STEEPEST DESCENT	$\hat{p}_k = \hat{p}_{k-1} + \mu_k H^T(\hat{p}_{k-1})R^{-1}(y - H(\hat{p}_{k-1})\hat{p}_{k-1})$
GAUSS-NEWTON	$\hat{p}_k = \hat{p}_{k-1} + \mu_k \left(H^T(\hat{p}_{k-1})R^{-1}H(\hat{p}_{k-1})\right)^{-1} H^T(\hat{p}_{k-1})R^{-1}(y - H(\hat{p}_{k-1})\hat{p}_{k-1})$

The 2×2 FIM $J(p)$ is defined as

$$J(p) = \mathrm{E}\left(\nabla_p^T \ln p_E(y - h(p))\nabla_p \ln p_E(y - h(p))\right) \tag{3a}$$

$$\nabla_p \ln p_E(y - h(p)) = \left(\frac{\mathrm{d}\ln p_E(y - h(p))}{\mathrm{d}X} \quad \frac{\mathrm{d}\ln p_E(y - h(p))}{\mathrm{d}Y}\right), \tag{3b}$$

where $p = (X, Y)$ is the 2-D position vector and $p_E(y - h(p))$ the likelihood given the error distribution.

In the case of Gaussian measurement errors $p_E(e) = \mathrm{N}(0, R(p))$, the FIM equals

$$J(p) = H^T(p)R(p)^{-1}H(p), \tag{4a}$$

$$H(p) = \nabla_p h(p). \tag{4b}$$

Table 5 summarizes the involved expressions for $h(p)$ and its gradient for RSS (Okumura-Hata model), TOA, TDOA, and AOA.

In the general case, for instance using (1c), numerical methods are needed to evaluate the CRLB. The larger the gradient $H(p^o)$, or the smaller the measurement error, the more information is provided from the measurement and the smaller the potential estimation error.

[TABLE 5] ANALYTICAL EXPRESSIONS RELATED TO SOME MEASUREMENTS AND GRADIENTS. [$\tilde{X}_i = X - X_i$, $\tilde{Y}_i = Y - Y_i$, $D_i = \sqrt{\tilde{X}_i^2 + \tilde{Y}_i^2}$. WITH SECTOR ANTENNAS, IT IS NOT LIKELY THAT DIRECTIONS ARE OBSERVED OUTSIDE $\alpha_i \pm 90°$, WHERE α_i IS THE DIRECTION OF THE ANTENNA MAIN LOBE.

METHOD	$h(p)$	$H(p) = \frac{dh(p)}{dp}$
RSS	$K + 10\alpha \ln_{10} D_i$	$\left(\frac{10\alpha}{\ln 10}\frac{\tilde{X}_i}{D_i^2}, \frac{10\alpha}{\ln 10}\frac{\tilde{Y}_i}{D_i^2}\right)$
TOA	D_i	$\left(\frac{\tilde{X}_i}{D_i}, \frac{\tilde{Y}_i}{D_i}\right)$
TDOA	$D_i - D_j$	$\left(\frac{\tilde{X}_i}{D_i} - \frac{\tilde{X}_j}{D_j}, \frac{\tilde{Y}_i}{D_i} - \frac{\tilde{Y}_j}{D_j}\right)$
AOA	$\alpha_i + \frac{180}{\pi}\arctan\frac{\tilde{Y}_i}{\tilde{X}_i}$	$\left(-\frac{\tilde{Y}_i}{D_i^2}\frac{180}{\pi}, \frac{\tilde{X}_i}{D_i^2}\frac{180}{\pi}\right)$
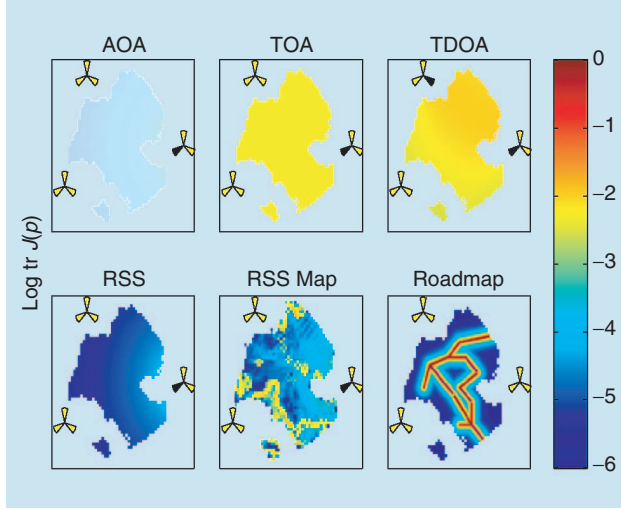
[FIG2] Spatial distribution of the scalar measure $\log_{10} J_{\mathrm{tr}}(p)$ in (5) for some central measurements relative to cell A (and cell B in case of TDOA) in the artificial network in Figure 1, using the error standard deviation from Table 2. For instance, the color corresponding to **−3** in the legend means that RMSE is larger than or equal to $\sqrt{10^3} \approx 30$ **meters** according to (7).

Information is additive, so if two measurements are independent, the corresponding information matrices can be added. This is easily seen from (4a) for $H^T = (H_1^T, H_2^T)$ and R being block diagonal, in which case we can write $J = J_1 + J_2$. Plausible approximate scalar information measures are the trace of the FIM and the smallest eigenvalue of FIM

$$J_{\mathrm{tr}}(p) \triangleq \mathrm{tr}J(p), \quad J_{\min}(p) \triangleq \min \mathrm{eig}\, J(p). \quad (5)$$

The former information measure is additive as FIM itself, while the latter is an underestimation of the information that is useful when reasoning about whether or not the available information is sufficient. Note that in the Gaussian case with a diagonal measurement error covariance matrix, the trace of FIM is the squared gradient magnitude. Figure 2 illustrates the information in the typical measurements in the artificial network of Figure 1 using the error standard deviations from Table 2. It is evident that RSS is the least informative, followed by AOA; TOA/TDOA is the most informative. The RSS map increases the information level to the same as AOA, and close to TOA/TDOA in some more informative areas. Road maps are the most informative, but are only applicable to road-bound mobility.

The CRLB is given by

$$\mathrm{Cov}(\hat{p}) = \mathrm{E}(p^o - \hat{p})(p^o - \hat{p})^T \geq J^{-1}(p^o), \quad (6)$$

where p^o denotes the true position. The CRLB holds for any unbiased estimate of $\hat{p}_t$, in particular the ones based on minimizing the criteria previously discussed. The lower bound may

not be an attainable bound. It is known that asymptotically in the information, the ML estimate is $\hat{p} \sim \mathrm{N}(p^o, J^{-1}(p^o))$ [38] and thus reaches this bound. Yet, this may not hold for a finite amount of inaccurate data.

The right-hand side of (6) gives an idea of how suitable a given sensor configuration is for positioning. It can also be used for system design (e.g., where to put the BSs or what information to include in the protocol standard). However, it should always be kept in mind that this lower bound is quite conservative and relies on many assumptions.

In practice, the root mean square error (RMSE) is perhaps of more importance. This can be interpreted as the achieved position error in meters. The CRLB implies the following bound:

$$\mathrm{RMSE} = \sqrt{\mathrm{E}\left[(X^o - \hat{X})^2 + (Y^o - \hat{Y})^2\right]}$$
$$\geq \sqrt{\mathrm{tr}\mathrm{Cov}(\hat{p})} \geq \sqrt{\mathrm{tr}J^{-1}(p^o)}. \quad (7)$$

The first inequality becomes an equality for unbiased estimates. If RMSE requirements are specified, it is possible to include more and more measurements in the design until (7) indicates that the amount of information is adequate. The circular error probability (CEP) defines a circular region for the RMSE, which is the measure specified by FCC (see Table 1 and the following section).

Another quantity relating to the CRB is the geometric dilution of precision (GDOP) often used in navigation applications. Basically, GDOP is the RMSE or CEP normalized with the measurement accuracy.

FCC REQUIREMENTS
To be more specific, we will now relate the CRLB to the FCC requirements. To compute the minimum information required in a very favorable case, we assume LOS, compute the ML estimate without getting stuck in a local minima, and assume the estimate follows its asymptotic distribution $\hat{p} \in \mathrm{N}(p^o, J^{-1}(p^o))$. In this case, we have $(\hat{p} - p^o)^T J^{-1} (p^o)(\hat{p} - p^o) \in \chi^2(2) = \exp(0.5)$. That is, the size of an ellipsoid for a given confidence level is found from the exponential distribution with explicit tail distribution $Q(x) = e^{-2x}$.

To squeeze this confidence ellipsoid in the FCC circle, we use the inequality below to compute the relation between confidence level $100\,\beta\%$ and the specified positioning error δ in meters

$$1 - \beta = P(|\hat{p} - p^o|^2 \geq \delta^2)$$
$$= P(J_{\min}(p^o)|\hat{p} - p^o|^2 \geq J_{\min}(p^o)\delta^2)$$
$$\leq P((\hat{p} - p^o)^T J^{-1}(p^o)(\hat{p} - p^o) \geq J_{\min}(p^o)\delta^2)$$
$$= e^{-2J_{\min}(p^o)\delta^2}$$
$$\Leftrightarrow J_{\min}(p^o) \geq \frac{2}{\delta^2} \ln\left(\frac{1}{1 - \beta}\right). \quad (8)$$

For the FCC requirements in Table 1, we get the minimum information [$J_{\min}(p^o)$] requirements according to Table 6.

Figure 3 illustrates the spatial distribution of $\log_{10} J_{\min}(p)$ for the different types of measurements (each case with a measurement triplet of relative cells A, B, and C). One conclusion is the TOA and TDOA are capable of meeting the FCC requirements with these assumptions, while RSS is not. It is also obvious that the RSS map increases the information in the RSS measurements, partly due to less measurement noise and partly due to larger variations in $h(p)$. AOA may meet the FCC requirements. The information can be further increased by using more measurements or using a digital road map for automotive applications.

NLOS PROBLEMS

All measures suffer from the problem of NLOS, causing positioning to become unreliable. This problem can be countered in two ways.

■ Use a robust error distribution. For instance, a TOA can have a heavy tail for positive errors as in (1c).
■ Include some logic in the search algorithm to rule out outliers.

See [39] for an initial discussion of NLOS problems and [40] and [41] for some algorithms in the second category.

A GEOMETRIC EXAMPLE

Consider the scenario in Figure 4, where four receivers are placed in the positions $(-1, 0)$, $(1, 0)$, $(0, -1)$, and $(0, 1)$. Each receiver measures the arrival time of a transmitted signal from an unknown position using accurate and synchronized clocks. If the transmitter is also synchronized, the signal propagation time can be computed, which leads to a TOA measurement. Propagation time corresponds to a distance, which leads to the distance circles around each receiver in Figure 4(a). If the transmitter is unsynchronized, each pair of receivers can compute a TDOA. This leads to a hyperbolic function where the transmitter can be located [42]. Four receivers can compute six such hyperbolic functions, which intersect in one unique point [see Figure 4(b)]. Some nice geometric interpretations are provided in [43] and [44]. Briefly, the intersection of the TDOA measurements can be seen as the intersection of unit cones from each transmitter. Further, the FIM can in the Gaussian case be seen as the second moment of unit vectors pointing at each BS.

Figure 4(c) and (d) shows the NLS loss functions corresponding to this scenario. For this particular scenario, the nonlinear equations have no local minima, so both a gradient and a Gauss-Newton algorithm should converge from any initial point.

The RMSE lower bounds from (7) for the TOA and TDOA measurements in this example are plotted in Figure 4(e) and

> **IN ESSENCE, POSITION ESTIMATION IS INTERPRETED AS A PROBLEM OF SOLVING SYSTEMS OF NONLINEAR EQUATIONS.**

(f). The level curves are scaled by σ_e, so a range error with standard deviation of 100 m will in the most favorable position lead to a position estimation error of 100 m. A bit counterintuitive, TDOA and TOA give the same performance close to the origin. To explain this, note that if all signals arrive simultaneously to all receivers, the transmission time does not add any information.

DYNAMIC CASE

MOTION MODELS

The key idea with filtering is to include the terminal velocity in a dynamic model, so a prediction of the next position can be computed. Depending on the context, the actual 2-D mobile velocity v_t might be completely unknown, partially known (Doppler shift), measurable (one example is a car-mounted system), or estimated in the model. The simplest possible motion models based on random walk, with or without velocity measurements, are summarized in Table 7. Any model suggested in the target tracking literature is also plausible for this application (see, for instance, the survey [45]). Here, we focus on the simplest cases. Higher order models can decrease estimation error slightly but will not drastically change our conclusions.
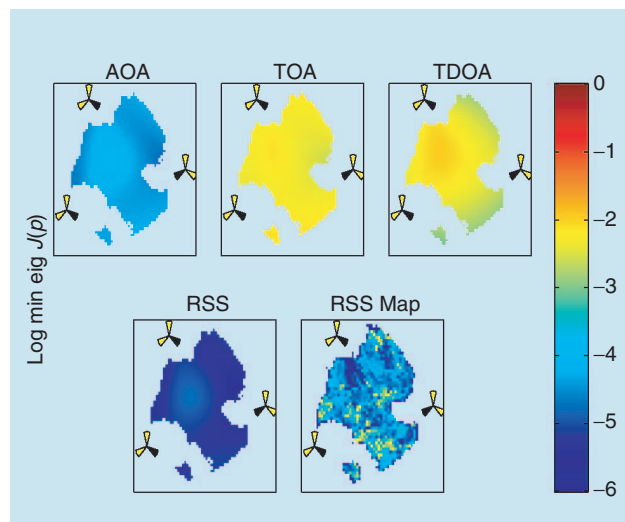
[FIG3] Spatial distribution of the minimum FIM eigenvalue $\log_{10}$ min eig $J(p)$ for measurements triplets relative cells A, B, and C in Figure 1, and noise error standard deviations from Table 2.

[TABLE 6] MINIMUM INFORMATION REQUIREMENTS BASED ON THE FCC POSITIONING REQUIREMENTS. [NOTE THAT FCC 1 IS THE DOMINATING REQUIREMENT WHEN A GAUSSIAN DISTRIBUTION IS ASSUMED.]

REQUIREMENT	NETWORK–CENTRIC	MOBILE–CENTRIC
FCC 1	$\log_{10} J_{\min}(p^o) \geq -3.7$	$\log_{10} J_{\min}(p^o) \geq -3.1$
FCC 2	$\log_{10} J_{\min}(p^o) \geq -4.2$	$\log_{10} J_{\min}(p^o) \geq -3.6$

The sample interval T_s determines the measurement update rate in the filter. Here, a bit of care is required since the measurements given in Table 2 are correlated over time while a filter requires uncorrelated measurements. The most immediate solution is to match the sample interval T_s to the coherence time of the measurements, which includes down-sampling (using an antialias filter) the measurements.

The measurement equation is still of the form $y_k = h(p_k) + e_k$ with the corresponding measurement FIM $J(p_k^o)$. The filtering CRLB depends on $J(p_k^o)$ but also on the motion model selection and the user mobility assumptions. Due to averaging effects, the bound will decrease considerably compared to the static case. Another advantage with temporal data and filtering compared to estimation in the static case is

> **MOBILE-CENTRIC SOLUTIONS ENABLE THE USE OF SAMPLED TEMPORAL MEASUREMENTS AND MOTION MODELS TO ENHANCE ESTIMATION ACCURACY AND INTEGRITY.**

that it is possible to handle an underdetermined equation system in the measurement equations.

As a possible improvement to the models in Table 7, the range to one BS may be introduced as an auxiliary state variable. Then, the TDOA measurements can be expressed linearly in the state vector and the problem with convergence to local minima is avoided.

Another way to obtain linear measurement relations to the models in Table 7 is to solve the static ML problem for each measurement and then use this position estimate $\hat{p}_k = \arg\min_p \ln p_E(y_k - h(p))$ and its approximate (asymptotic) distribution $\hat{p}_k \in N(p, J^{-1}(p))$ as the measurement relation. The position estimate here acts as a sufficient statistic for the available information.
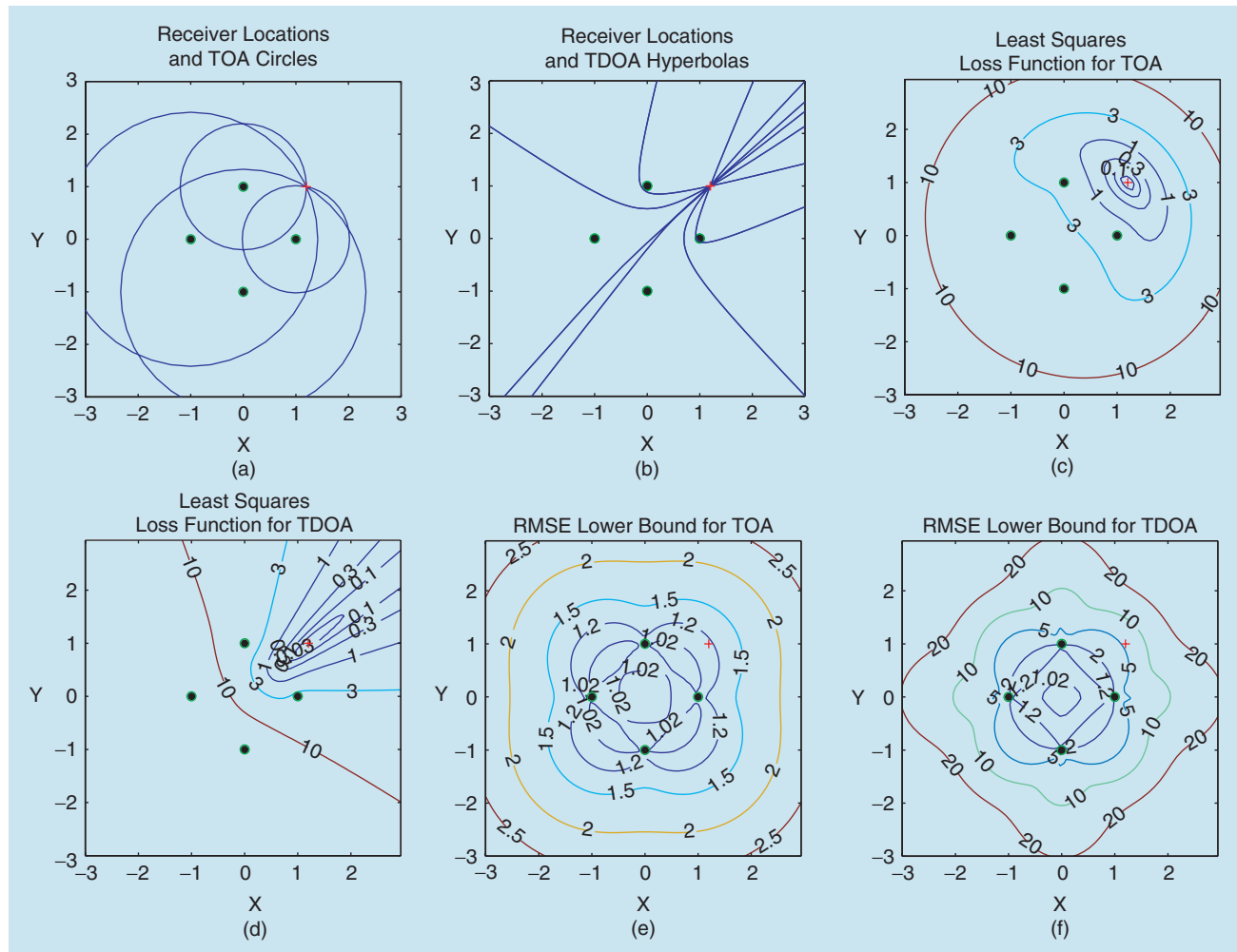
[FIG4] (a) and (b): Example scenario with four receivers are placed in a square, and there is one transmitter at (1.2,1). With TOA measurements, each receiver measurement constrains the transmitter position to a circle. With TDOA measurements, each *pair of* receive measurements constrains the transmitter position to a hyperbola. (c) and (d): Nonlinear least squares (NLS) loss functions, or the negative log likelihood for Gaussian error distribution, for TOA and TDOA measurements, respectively. (e) and (f): RMSE lower bound implied by the CRLB measurements for TOA and TDOA, respectively. The unit is scaled to the measurement standard deviation.

POSITION FILTERING

The simplest approach would be to use adaptive filters similar to the numerical search schemes in Table 4. An adaptive algorithm based on the steepest descent principle is the least mean square (LMS) algorithm. Similarly, the recursive least squares (RLS) algorithm is an adaptive version of a Gauss-Newton search. The tuning parameter μ or λ controls the amount of averaging and reflects our belief in user mobility rate.

The last two models M3 and M4 in Table 7 require state estimation. The natural first attempt is the extended Kalman filter (EKF), in which measurement errors are assumed Gaussian and the nonlinear measurement equation $y_k = h(p_k) + e_k$ is linearized around the current position estimate. In case of a highly nonlinear measurement equation $h(p_k)$, or non-Gaussian error distribution, the position estimate using the EKF is far from the CRLB. The computer-intensive particle filter (PF) [46], [47] has been proposed for high-performance positioning [15]. The advantage is that all currently available information described in the section on measurements is easily incorporated, including power attenuation maps and street maps. Some examples are provided in [48].

FUNDAMENTAL PERFORMANCE BOUNDS

Recently, location performance in the dynamic case in terms of the CRLB has been studied in [49]–[51] for the TDOA case. Remember that the CRLB is asymptotic in the information, and thus it is a conservative bound also in filtering. The CRLB for nonlinear filtering was derived in [52]. In short, they presented a recursion for nonlinear models similar to the information filter version of the Riccati equation that computes a lower estimation bound P_k. We here present a general result for the random walk model M1 and velocity sensor model M2 in Table 7. With process noise covariance matrix $\text{Cov}(w_k) = Q_k$, both result in the same recursion

$$\text{Cov}(p_k) \geq P_k, \tag{9a}$$

$$P_{k+1} = \left((P_k + T_s Q_k)^{-1} + J(p_k^o) \right)^{-1}. \tag{9b}$$

In the cases of M3 and M4 with a velocity state in Table 7, define $H = (I, 0)$. This yields

$$\text{Cov}(p_k) \geq H P_k H^T, \tag{10a}$$

$$P_{k+1} = \left((F P_k F^T + G Q_k G^T)^{-1} + H^T J(p_k^o) H \right)^{-1}. \tag{10b}$$

These expressions clearly show the compromise between mobility (Q) and information (J). Later in this article, a few specific cases of special interest will be pointed out.

The position-dependent information matrix $J(p^o)$ is under mild conditions on the measurement relation $h(p)$ a smooth function and can be considered constant for movements in a small neighborhood of p^o. The Riccati recursion will then converge to a stationary point. We will in the sequel analyze the first two cases in Table 7 in more detail. For (9b), the stationary value is given by

$$\bar{P} = \left((\bar{P} + T_s Q)^{-1} + J(p^o) \right)^{-1}, \tag{11}$$

which has the solution (see "Stationary Riccati Equation for Positioning")

$$\bar{P} = -\frac{1}{2} T_s Q + J^{-1/2}(p^o)$$
$$\times \left(J^{1/2}(p^o)(T_s Q + \frac{T_s^2}{4} Q J Q) J^{1/2}(p^o) \right)^{1/2} J^{-1/2}(p^o). \tag{12}$$

The following procedure thus yields the bound for any wireless positioning application.

1) Select measurements from Table 2.
2) Compute the FIM using (4a) and (4b).
3) Select a motion model (random walk M1 or velocity sensor model M2) from Table 7.
4) Compute (12).

We can also point out a couple of important special cases.

■ For the case with large mobility uncertainty, $Q \to \infty$ and (11) gives $P_k = J^{-1}(p^o)$, which is the static case.

■ For the case of symmetric movements in more than one dimension, we can assume that $Q = qI$. The measurement equation can also be assumed to be symmetric in the different dimensions (it can always be transformed to this form anyway), which means $J = J_{\min}(p^o)I$. This assumption can also

M1: RANDOM WALK MODEL	$p_{k+1} = p_k + T_s w_k$
M2: VELOCITY SENSOR MODEL	$p_{k+1} = p_k + T_s v_k + T_s w_k$
M3: RANDOM FORCE MODEL	$\begin{pmatrix} p_{k+1} \\ v_{k+1} \end{pmatrix} = \underbrace{\begin{pmatrix} I & T_s \cdot I \\ 0 & I \end{pmatrix}}_{F} \begin{pmatrix} p_k \\ v_k \end{pmatrix} + \underbrace{\begin{pmatrix} T_s^2/2 \cdot I \\ T_s \cdot I \end{pmatrix}}_{G} w_k$
M4: INERTIAL SENSOR MODEL	$\begin{pmatrix} p_{k+1} \\ v_{k+1} \end{pmatrix} = \begin{pmatrix} I & T_s \cdot I \\ 0 & I \end{pmatrix} \begin{pmatrix} p_k \\ v_k \end{pmatrix} + \begin{pmatrix} T_s^2/2 \cdot I \\ T_s \cdot I \end{pmatrix} a_k + \begin{pmatrix} T_s^2/2 \cdot I \\ T_s \cdot I \end{pmatrix} w_k$

[TABLE 8] RANDOM WALK MOTION PARAMETER q AND ITS CORRESPONDING MOTION STATE USED FOR ILLUSTRATION. MINIMUM INFORMATION $\log_{10}(J_{min})$ NEEDED IN EACH CASE USING (12) TO REACH THE FCC REQUIREMENTS IN TABLE 1 IN A FAVORABLE SITUATION, ASSUMING $T_s = 1$s. THE APPROXIMATION (15B) GIVES THE SAME RESULT EXCEPT FOR A SMALL DISCREPENCY FOR THE LAST TWO VALUES.						
MOBILITY	MOTION STATE	$\sqrt{q}$ [M/S]	FCC-N 1	FCC-N 2	FCC-M 1	FCC-M 2
STAND-STILL	1	0	$-\log_{10}(k) - 3.7$	$-\log_{10}(k) - 4.2$	$-\log_{10}(k) - 3.1$	$-\log_{10}(k) - 3.6$
INDOOR	2	0.3	-8.4	-9.4	-7.2	-8.2
WALKING	3	3	-6.4	-7.4	-5.2	-6.2
CAR	4	30	-4.4	-5.4	-3.4	-4.3

be seen as a conservative circular bound on the confidence ellipsoid. Then, the asymptotic CRLB according to (12) is

$$\bar{P} = \frac{qT_s}{2} \left(\sqrt{\frac{4}{J_{\min}(p^o)qT_s} + 1} - 1 \right) I \tag{13a}$$

$$\approx \begin{cases} \frac{1}{J_{\min}(p^o)} I & \text{if } \frac{J_{\min}(p^o)qT_s}{4} \gg 1 \\ \sqrt{\frac{qT_s}{J_{\min}(p^o)}} I & \text{if } \frac{J_{\min}(p^o)qT_s}{4} \ll 1. \end{cases} \tag{13b}$$

The second case is the normal case, as will be apparent when plugging in realistic values. The first case of very rapid movements and/or very informative measurements corresponds to the static case.

■ For the special case of no movement at all ($Q = 0$), the solution is found from (9b) directly (assuming $P_0^{-1} = 0$) as

$$P_k = \frac{1}{k} J^{-1}(p^o) = \frac{T_s}{t} J^{-1}(p^o). \tag{14}$$

This case is of interest for MS equipped with a stand-still detector (available in some models today for energy-saving purposes).

FCC REQUIREMENTS
It is interesting to establish the relation between the FCC requirements in Table 1 and the benefits from filtering. A sensor configuration that fails the FCC requirements in the static case might satisfy the requirements if a sufficient gain from filtering is present. Consider the case in the previous section with less informative measurements or very limited movements. After a similar motivation to that seen in the earlier "FCC Requirements" section with the same circular positioning error distribution assumption, (8) becomes

$$\frac{1}{\sqrt{\frac{qT_s}{J_{\min}(p^o)}}} \geq \frac{2}{\delta^2} \ln\left(\frac{1}{1-\beta}\right), \tag{15a}$$

$$J_{\min}(p^o) \geq \frac{qT_s}{\left(\frac{\delta^2}{2\ln(1-\beta)}\right)^2}. \tag{15b}$$

This constitutes an explicit bound on the information, and also an implicit upper limit on q to make a certain sensor con-

figuration meet the FCC requirements formulated as the right hand side of (15). Table 8 exemplifies the information needed for three typical velocity intervals in a random walk model M1. As seen, considerably less information is needed compared to the static case (8). We also note that the assumption in the Taylor expansion in (13a) is valid for $\log_{10}(J_{\min})$ approximately less than -3, even in the car mobility case where $\text{Var}(w_k) = q = 30^2$.

In the special case of no movement at all, (8) and (14) combine to the information requirement

$$J_{\min}(p^o) \geq \frac{2}{k\delta^2} \ln\left(\frac{1}{1-\beta}\right). \tag{16}$$

The static case is obtained with $k = 1$, so the standstill case in Table 8 with $\log_{10}(1) = 0$ corresponds to the values in Table 6.

The value of the random walk noise variance q is usually considered as a design parameter in model-based filtering. The values chosen in Table 8 are merely for illustration purposes. In light of how many measurements are required in the standstill case to reach the other motion states, one may argue that q should be increased an order of magnitude. However, we leave this as a design issue and conclude that, in any way, the required information is potentially relaxed at least an order of magnitude by filtering the measurements compared to a snap-shot approach.

A SIMPLE FILTERING EXAMPLE
The following simplified positioning example illustrates the interplay of true and modeled motion. The random walk model M1 in one dimension is given by

$$p_{k+1} = p_k + w_k \tag{17}$$
$$y_k = p_k + e_k. \tag{18}$$

The example can be generalized to independent motions in two and three dimensions. We assume an A-GPS measurement with sampling frequency 1 Hz and with Gaussian error with standard deviation 10 m ($\sigma_e^2 = 10^2$). It is further assumed that all other information can be neglected when A-GPS is available. The true motion corresponds to one of the cases 2–4 in Table 8. Note that without an explicit velocity state, the model implies that a walking user may change velocity from 3 m/s forwards to 3 m/s backwards in 1 s.

Now, the actual motion is not known, and the problem is to design one process noise covariance matrix $\text{Cov}(w_k) = Q = qI$ that gives good overall performance. Figure 5 shows the RMSE in meters. The plot reveals that it is safer to overestimate mobility than to underestimate it. The worst thing that can happen is that we come back to the static case, that is RMSE $= \sigma_e = 10$ m. On the other hand, if we knew that the transmitter is not moving faster than 0.3 m/s, then the RMSE can be as low as 2.5 m. Note that some MS today are equipped with motion detectors for energy-saving modes, which can be used to advantage here.

This example is linear and Gaussian, so the Kalman filter attains the CRLB in (13a), which is also plotted in Figure 5 for comparison.

SUPPORT SENSORS FOR FILTERING

The performance can be substantially increased using velocity sensors or inertial sensors as accelerometers and gyroscopes. Today, these are available for cost and space-efficient mass production with fair accuracy. Suppose first that it is possible to measure the velocity vector directly. This implies that the velocity sensor model M2 in Table 7 is applicable, and the velocity measurement error becomes the random walk input w_k. That is, if the velocity error has standard deviation 0.3, then $q = 0.3^2$ should be used independent of the actual speed. Clearly, the information requirement can be released then for fast mobility. This effectively means that we switch from one curve in Figure 5(a) to another one below it, since we have a much smaller q^o, and the potential RMSE decreases according to Figure 5(b). We can here read off the required velocity quality for a specified performance.

FILTER BANK TECHNIQUES

There will be an increase in automotive telematic systems in the future. As such, related services will emerge. For that reason, the positioning system should try to detect whether the user is traveling by car. Similarly, walking and indoor users may be detected for increased performance. Consider a discrete motion state $m \in \mathcal{Z}$, as illustrated in Table 8. If an oracle provides this state, the Kalman fil-

ter can be adapted to this motion model and the performance gain in Figure 5(b) is obtained. In some cases, the positioning system may know the motion state, for instance from the connection to an automotive docking station or from the fact that the user is connected to an indoor BS. Otherwise, it is plausible to use one adaptive filter from Table 8 with different models or with different values on the motion parameter (see Table 8): Q for EKF and PF, step size for LMS, or forgetting factor for RLS.

There are plenty of principles that dictate how to combine the outputs of these filters to one position estimate, for instance merging the states as in interactive multiple models (IMM), pruning as in adaptive forgetting through multiple models (AFMM), or motion parameter estimation as in hidden Markov models (HMM) (see [53] for an overview). A performance lower bound when the number of states increases is the CRLB in Figure 5(b) as a function of true mobility.

> WE DISCUSS AND ILLUSTRATE POSSIBILITIES AND FUNDAMENTAL LIMITATIONS ASSOCIATED WITH MOBILE POSITIONING, BASED ON AVAILABLE WIRELESS NETWORK MEASUREMENTS.
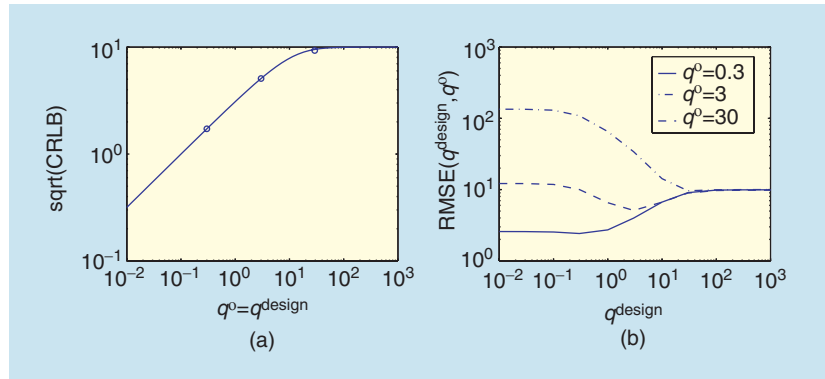
[FIG5] (a) Resulting RMSE as a function of true transmitter mobility q^o and design parameter q^{design}. (b) The CRLB as a function of q^o, which in this case is attainable for the Kalman filter with $q^{\text{design}} = q^o$. The circles denote the three cases of q^o to the right.

[TABLE 9] ADAPTIVE FILTERS APPLICABLE TO THE DYNAMIC MOTION MODELS IN TABLE 7. [THE LEAST MEAN SQUARE (LMS) AND RECURSIVE LEAST SQUARES (RLS) ALGORITHMS ARE APPLICABLE TO THE FIRST TWO MODELS, M1 AND M2, IN TABLE 7. THE EXTENDED KALMAN FILTER (EKF) AND PARTICLE FILTER (PF) APPLY TO MORE GENERAL MODELS, INCLUDING M1–M4.]

LMS	$\hat{p}_k = \hat{p}_{k-1} + \mu H^T(\hat{p}_{k-1})(y_k - H(\hat{p}_{k-1})\hat{p}_{k-1})$
RLS	$\hat{p}_k = \hat{p}_{k-1} + P_k H^T(\hat{p}_{k-1})(y_k - H(\hat{p}_{k-1})\hat{p}_{k-1})$
	$P_k = \frac{1}{\lambda}\left(P_{k-1} - P_{k-1}H^T(\hat{p}_{k-1})\left(\lambda R_k + H(\hat{p}_{k-1})P_{k-1}H^T(\hat{p}_{k-1})\right)^{-1}H(\hat{p}_{k-1})P_{k-1}\right)$
EKF	$\hat{p}_k = \hat{p}_{k-1} + P_{k|k-1}H^T(\hat{p}_{k-1})(y_k - H(\hat{p}_{k-1})\hat{p}_{k-1})$
	$P_{k|k} = P_{k|k-1} - P_{k|k-1}H^T(\hat{p}_{k-1})\left(R_k + H(\hat{p}_{k-1})P_{k|k-1}H^T(\hat{p}_{k-1})\right)^{-1}H(\hat{p}_{k-1})P_{k|k-1}$
	$P_{k+1|k} = FP_{k|k}F^T + GQ_kG^T$
PF	INITIALIZE N PARTICLES p_0^i, $i = 1, 2, \ldots, N$. FOR EACH TIME t:
	1) LIKELIHOOD COMPUTATION $\pi^i = p_E(y_k - h(p_k^i))$.
	2) RESAMPLE N PARTICLES WITH REPLACEMENT ACCORDING TO LIKELIHOOD WEIGHT π^i.
	3) DIFFUSION STEP: RANDOMIZE w^i FROM p_w AND LET $p_{k+1}^i = Fp_k^i + Gw^i$.

CONCLUSIONS

Location in wireless networks is of increasing importance for safety, gaming, and commercial services. There are plenty of measurements available today, ranging from signal arrival times to maps of received power. We have demonstrated how fundamental the FIM for each measurement is to assess possible location performance. As one illustration, the FCC positioning requirements are transformed to requirements on sufficient information. Thereby, it is possible to investigate whether specific sensor configurations would provide acceptable accuracy. The information is additive, so several measurements increase information. The information concept can also handle less conventional measurements, such as digital propagation prediction maps and road maps. A practical question is whether there is an algorithm that attains the position error lower bound and if it is possible to implement this algorithm in practice. This, of course, depends from case to case, and we have briefly pointed out algorithms of particular interest.

A short road path to implement a positioning system is as follows.

- 1) Collect the available measurements in Table 2.
- 2) Compute the static CRB using (3) or using (4a) in the Gaussian case.
- 3) Compare this to the FCC requirements in Table 1.
- 4) If these are not satisfied, continue with step 5. Otherwise, evaluate algorithms based on one of the criteria in Table 3 using one of the algorithms in Table 4. If these algorithms do not yield a satisfactory result, continue with step 5.
- 5) Select a motion model in Table 7.
- 6) Compare the CRB to the FCC requirements in Table 8.
- 7) If these are satisfied, try to find an algorithm in Table 9 that gives satisfactory result. If this fails, try to change the system configuration to obtain better measurements, or equip the MS with more sensors.

Briefly, the results indicate that the FCC requirement may be reached using a snapshot localization approach in a most favorable situation, including LOS and a good estimator. The accuracy is increased an order of magnitude with filtering and potentially another order of magnitude with motion sensors.

ACKNOWLEDGMENTS

AUTHORS

Fredrik Gustafsson is professor in communication systems at the Department of Electrical Engineering at Linkaping University, Sweden. He received the M.S. degree in electrical engineering in 1988 and the Ph.D. degree in automatic control in 1992, both from Linkoping University. His research is focused on statistical signal processing, with applications to automotive, avionics, and communication systems. He is an associate editor of *IEEE Transactions of Signal Processing*.

Fredrik Gunnarsson is a senior research engineer at Ericsson Research and a research associate at Linköping University, Sweden. He received the M.Sc. degree in 1996 and the Ph.D. degree in 2000, both in electrical engineering, from Linkoping University. His research interests include radio resource management and signal processing for wireless communications.

REFERENCES

[1] J.J. Caffery and G.L. Stuber, "Overview of radiolocation in CDMA cellular systems," *IEEE Commun. Mag.*, vol. 36, no. 4, pp. 38–45, Apr. 1998.

[2] Y. Zhao, "Standardization of mobile phone positioning for 3G systems," *IEEE Commun. Mag.*, vol. 40, no. 7, pp. 108–116, July 2002.

[3] C. Drane, M. Macnaughtan, and C. Scott. "Positioning GSM telephones," *IEEE Commun. Mag.*, vol. 36, no. 4, pp. 46–54, Apr. 1998.

[4] G. Sun, J. Chen, W. Guo, and K.J.R. Liu, "Signal processing techniques in network-aided positioning," *IEEE Signal Processing Mag.*, vol. 22, no. 4, pp. 12–23, July 2005.

[5] A.H. Sayed, A. Tarighat, and N. Khajehnouri, "Network-based wireless location," *IEEE Signal Processing Mag.*, vol. 22, no. 4, pp. 24–40, July 2005.

[6] K. Pahlavan, L. Xinrong, and J.-P. Mäkelä, "Indoor geolocation science and technology" *IEEE Commun. Mag.*, vol. 40, no. 2, pp. 112–118, Feb. 2002.

[7] S. Gezici, Z. Tian, G.B. Giannakis, H. Kobayashi, A.F. Molish, H.V. Poor, and Z. Sahinglu, "Localization via ultra-wideband radios," *IEEE Signal Processing Mag.*, vol. 22, no. 4, pp. 70–84, July 2005.

[8] N. Patwari, A.O. Hero III, J. Ash, R.L. Moses, S. Kyperountas, and N.S. Correal, "Locating the nodes," *IEEE Signal Processing Mag.*, vol. 22, no. 4, pp. 54–69, July 2005.

[9] D.N. Hatfield, "A report on technical and operational issues impacting the provision of wireless enhanced 911 services," Federal Communications Commission, Tech. Rep., 2002.

[10] J.J. Caffery, *Wireless Location in CDMA Cellular Radio Systems*. Norwell, MA: Kluwer, 1999.

[11] Y. Zhao, "Overview of 2G LCS technologies and standards," in *Proc. 3GPP TSG SA2 LCS Workshop*, London, UK, Jan. 2001.

[12] K.J. Krizman, T.E. Biedka, and T.S. Rappaport, "Wireless position location: Fundamentals, implementation strategies, and sources of error," in *Proc. IEEE Vehicular Technology Conf.*, June 1997, vol. 2, pp. 919–923.

[13] Y. Okumura, E. Ohmori, T. Kawano, and K. Fukuda, "Field strength and its variability in VHF and UHF land-mobile radio service," *Rev. Elec. Commun. Lab.*, vol. 16, pp. 9–10, 1968.

[14] M. Hata, "Empirical formula for propagation loss in land mobile radio services," *IEEE Trans. Veh. Technol.*, vol. 29, no. 3, pp. 317–325 1980.

[15] F. Gustafsson, F. Gunnarsson, N. Bergman, U. Forssell, J. Jansson, R. Karlsson, and P-J. Nordlund, "Particle filters for positioning, navigation and tracking," *IEEE Trans. Signal Processing*, vol. 50, no. 2, pp. 425–437, Feb. 2002.

[16] R. Karlsson and F. Gustafsson, "Particle filter and Cramér-Rao lower bound for underwater navigation," in *Proc. IEEE Conf. Acoustics, Speech and Signal Processing (ICASSP)*, Hong Kong, China, Apr. 2003, vol. 6, pp. 65–68.

[17] M.C. Vanderveen, A.-J. van der Veen, and A. Paulraj, "Estimation of multipath parameters in wireless communications," *IEEE Trans. Signal Processing*, vol. 46, pp. 682–290, Mar. 1998.

[18] C. Botteron, A. Host-Madsen, and M. Fattouche, "Cramér-Rao bound for location estimation of a mobile in asynchronous DS-CDMA systems," in *Proc. IEEE Conf. Acoustics, Speech and Signal Processing*, Salt Lake City, UT, May 2001, vol. 4, pp. 2221–2224.

[19] E. Ström and F. Malmsten,"A maximum likelihood approach for estimating DS-CDMA multipath fading channels," *IEEE J. Select. Areas Commun.,* vol. 18,, no. 1, pp. 132–140, Jan. 2000.

[20] H. Koorapaty, "Cramer-Rao bounds for time of arrival estimation in cellular systems," in *Proc. IEEE Vehicular Technology Conf.*, Milan, Italy, May 2004, vol. 5, pp. 2729–2733.

[21] G.G. Raleigh and T. Boros, "Joint space-time parameter estimation for wireless communication channels," *IEEE Trans. Signal Processing*, vol. 46, pp. 1333–1343, May 1998.

[22] Y.Qi and H. Kobayashi, "On relation among time delay and signal strength based geolocation methods," in *Proc. IEEE Global Telecommunications Conf.*, San Francisco, CA, Dec. 2003, pp. 4079–4083.

[23] A.J. Weiss, "On the accuracy of a cellular location system based on received signal strength measurements," *IEEE Trans. Veh. Technol.*, vol. 52, no. 6, pp. 1508–1518, June 2003.

[24] G. Hendeby and F. Gustafsson, "Fundamental filtering limitations in linear non-gaussian systems," in *Proc. IFAC World Congress (IFAC'05)*, Prague, July 2005.

[25] J.O. Smith and J.S. Abel, "Closed-form least-squares source location estimation from range-difference measurements," *IEEE Trans. Acoustics, Speech, Signal Processing*, vol. 35, pp. 1661–1669, 1987.

[26] J.E. Dennis, Jr. and B. Schnabel, *Numerical Methods for Unconstrained Optimization and Non-linear Equations* (Prentice-Hall Series in Computational Mathematics). Englewood Cliffs, NJ: Prentice-Hall, 1983.

[27] A. Urruela and J. Riba, "Novel closed-form ML position estimator for hyperbolic location," in *Proc. IEEE Conf. Acoustics, Speech and Signal Processing*, Montreal, Canada, May 2004, vol. 2, pp. 149–152.

[28] F. Gustafsson and F. Gunnarsson, "Positioning using time-difference of arrival measurements," in *Proc. IEEE Conf. Acoustics, Speech and Signal Processing (ICASSP)*, Hong Kong, China, Apr. 2003, vol. 6, pp. 553–556.

[29] S.M. Kay, *Fundamentals of Signal Processing—Estimation Theory*. Englewood Cliffs, NJ: Prentice Hall, 1993.

[30] C. Botteron, A. Host-Madsen, and M. Fattouche, "Effects of system and environment parameters on the performance of network-based mobile station position estimators," *IEEE Trans. Veh. Technol.*, vol. 53, no. 1, pp. 163–180, Jan. 2004.

[31] C. Botteron, A. Host-Madsen, and M. Fattouche, "Cramer-Rao bounds for the estimation of multipath parameters and mobiles' positions in asynchronous DS-CDMA systems," *IEEE Trans. Signal Processing*, vol. 52, no. 4, pp. 862–875, Jan. 2004.

[32] C. Botteron, M. Fattouche, and A. Host-Madsen, "Statistical theory of the effects of radio location system design parameters on the position performance," in *Proc. IEEE Vehicular Technology Conf.*, Vancouver, Canada, Sept. 2002, pp. 1187–1191.

[33] N. Patwari, A.O. Hero III, M. Perkins, N.S. Correal, and R.J. O'Dea, "Relative location estimation in wireless sensor networks," *IEEE Trans. Signal Processing*, vol. 51, no. 8, pp. 2137–2148, Aug. 2003.

[34] H. Koorapaty, H. Grubeck, and M. Cedervall, "Effect of biased measurement errors on accuracy of position location methods," in *Proc. IEEE Global Telecommunications Conf.*, Sydney, Australia, Nov. 1998, pp. 1497–1502.

[35] H. Koorapaty, "Barankin bound for position estimation using received signal strength measurements," in *Proc. IEEE Vehicular Technology Conf.*, Milan, Italy, May 2004, pp. 2686–2690.

[36] Y. Qi and H. Kobayashi, "On geolocation accuracy with prior information in non-line-of-sight environment," in *Proc. IEEE Vehicular Technology Conf.*, Vancouver, Canada, Sept. 2002, pp. 285–288.

[37] Y.Qi and H. Kobayashi, "Cramer-Rao lower bound for geolocation in non-line-of-sight environment," in *Proc. IEEE Conf. Acoustics, Speech and Signal Processing*, Orlando, FL, May 2002, pp. 2473–2476.

[38] E.L. Lehmann, *Theory of Point Estimation* (Statistical/Probability Series). Belmont, CA: Wadsworth & Brooks/Cole, 1991.

[39] M.P. Wylie and J. Holtzman, "The non-line-of-sight problem in mobile location estimation," in *Proc. IEEE Int. Conf. Universal Personal Communications*, Oct. 1996, pp. 827–831.

[40] J. Riba and A. Urruela, "A non-line-of-sight mitigation technique based on ML-detection," in *Proc. IEEE Conf. Acoustics, Speech and Signal Processing*, Montreal, Canada, May 2004, vol. 2, pp. 153–156.

[41] J. Zhen and S. Zhang, "Adaptive AR model based robust mobile location estimation approach in NLoS environment," in *Proc. IEEE Vehicular Technology Conf.*, Milan, Italy, May 2004, pp. 2682–2685.

[42] B.T. Fang, "Simple solutions for a hyperbolic and related position fixes," *IEEE Trans. Aerospace and Electronic Systems*, vol. 26, no. 5, pp. 748–753, Sept. 1990.

[43] J.S. Abel and J. Chaffee, "Integrating ranging transponders with GPS," in *Proc. 1991 ION Nat. Technical Meeting*, Phoenix, AZ, 1991, pp. 15–24.

[44] J.S. Abel and J. Chaffee, "The geometry of GPS solutions," in *Proc. 1992 Institute of Navigation Nat. Technical Meeting*, San Diego, CA, 1992, pp. 425–430.

[45] X.R. Li and V.P. Jilkov, "Survey of maneuvering target tracking. Part I: Dynamic models," *IEEE Trans. Aerosp. Electron. Syst.*, vol. 39, no. 4, pp. 1333–1364, 2003.

[46] N.J. Gordon, D.J. Salmond, and A.F.M. Smith, "A novel approach to nonlinear/non-Gaussian Bayesian state estimation," *IEE Proc. Radar Signal Processing*, vol. 140, pp. 107–113, 1993.

[47] A. Doucet, N.D. Freitas, and N. Gordon, Eds., *Sequential Monte Carlo Methods in Practice*. New York: Springer-Verlag, 2001.

[48] P-J. Nordlund, F. Gunnarsson, and F. Gustafsson, "Particle filters for positioning in wireless networks," in *Proc. European Signal Processing Conf. (EUSIPCO)*, Toulouse, France, Sept. 2002, pp. 311–314.

[49] A. Urruela and J. Riba, "A novel estimator and performance bound for time propagation and Doppler based radio-location," in *Proc. IEEE Conf. Acoustics, Speech and Signal Processing*, Hong Kong, China, Apr. 2003, vol. 5, pp. 253–256.

[50] A. Urruela and J. Riba, "A novel estimator and theoretical limits for in-car radio-location," in *Proc. IEEE Vehicular Technology Conf.*, Orlando, FL, Oct. 2003, pp. 747–751.

[51] A. Urruela and J. Riba, "Efficient mobile location from time measurements with unknown variances in dynamic scenarios," in *Proc. IEEE Workshop Signal Processing Advances in Wireless Communications*, Lisbon, Portugal, July 2004, pp. 1522–1526.

[52] N. Bergman, "Posterior Cramér-Rao bounds for sequential estimation," in *Sequential Monte Carlo Methods in Practice,* A. Doucet, N. de Freitas, and N. Gordon, Eds. New York: Springer-Verlag, 2001, pp. 321–338.

[53] F. Gustafsson, *Adaptive Filtering and Change Detection*. New York: Wiley, 2000.

APPENDIX
STATIONARY RICCATI EQUATION FOR POSITIONING

Equation (11) can be rewritten first by removing the matrix inversions and then by completing the squares

$$\bar{P}^{-1} = (\bar{P} + Q)^{-1} + J(p^o) \tag{19a}$$

$$\Rightarrow \bar{P}J(p^o)\bar{P} + QJ(p^o)\bar{P} = Q \tag{19b}$$

$$\Rightarrow \left(\bar{P}J^{1/2}(p^o) + \frac{1}{2}QJ^{1/2}(p^o) \right)$$
$$\times \left(J^{1/2}(p^o)\bar{P} + \frac{1}{2}J^{1/2}(p^o)Q \right)$$
$$= Q + \frac{1}{4}QJQ \tag{19c}$$

$$\Rightarrow \left(J^{1/2}(p^o)\bar{P}J^{1/2}(p^o) + \frac{1}{2}J^{1/2}(p^o)QJ^{1/2}(p^o) \right)$$
$$\times \left(J^{1/2}(p^o)\bar{P}J^{1/2}(p^o) + \frac{1}{2}J^{1/2}(p^o)QJ^{1/2}(p^o) \right)$$
$$= J^{1/2}(p^o)\left(Q + \frac{1}{4}QJQ \right)J^{1/2}(p^o) \tag{19d}$$

$$\Rightarrow \bar{P} = -\frac{1}{2}Q + J^{-1/2}(p^o)$$
$$\times \left(J^{1/2}(p^o)(Q + \frac{1}{4}QJQ)J^{1/2}(p^o) \right)^{1/2} J^{-1/2}(p^o). \tag{19e}$$

All involved matrices are symmetric, so it follows from (19b) that $QJ(p^o)\bar{P}$ is also symmetric, a fact used in the factorization (19c). The left and right multiplication with $J^{1/2}(p^o)$ in (19d) is done to achieve a symmetric solution for $\bar{P}$. We have found one symmetric positive semidefinite solution, and we know from the general Riccati theory that the solution is unique. Hence, we are done. **SP**